Chemical Engineering Journal 151 (2009) 1–9

Contents lists available at ScienceDirect

Chemical Engineering Journal

journal homepage: www.elsevier.com/locate/cej

Review

Characteristics of pseudo-second-order kinetic model for liquid-phase adsorption: A mini-review

Feng-Chin Wu[a,*], Ru-Ling Tseng[b], Shang-Chieh Huang[b], Ruey-Shin Juang[c,d]

[a] Department of Chemical Engineering, National United University, Miao-Li 360, Taiwan
[b] Department of Safety, Health and Environmental Engineering, National United University, Miao-Li 360, Taiwan
[c] Department of Chemical Engineering and Materials Science, Yuan Ze University, Chung-Li 32003, Taiwan
[d] Fuel Cell Center, Yuan Ze University, Chung-Li 32003, Taiwan

ARTICLE INFO

Article history:
Received 14 July 2008
Received in revised form
25 December 2008
Accepted 22 February 2009

Keywords:
Adsorption
Kinetic model
Approaching equilibrium factors
Rate index
Activated carbon

ABSTRACT

Since the introduction of pseudo-second-order (PSO) model for the description of adsorption kinetics in 1999, it has been widely applied in liquid-phase adsorption systems. An approaching equilibrium factor (R_w) was defined and deduced from the PSO model in this work. The adsorption characteristic curves were built up, in which three different zones of the PSO model were classified. Activated carbons with various particle sizes were prepared from fir wood with KOH activation for the adsorption of phenol, 4-chlorophenol (4-CP), 2,4-dichlorophenol (2,4-DCP), 2,4,6-trichlorophenol (2,4,6-TCP), and methylene blue (MB) from water. Suitable ranges of the PSO model and the effect of adsorbent particle size on the R_w value were analyzed. It was found that the quantity k_2q_e was exactly the inverse of the half-life of adsorption process. It could be used as an indicator of kinetic performance because it was a key parameter affecting the fractional adsorption at any time. That is, k_2q_e, a newly defined rate index, could provide the related information between the static and dynamic behavior of adsorption processes in engineering practice.

1. Introduction

The simple linear equation of a pseudo-second-order (PSO) model for the analysis of adsorption kinetic data has been deduced by Ho and McKay [1–5]. Literature survey has roughly shown that the number of publications referring to other kinetic models such as the pseudo-first-order model, intraparticle diffusion (IPD) model, and Elovich equation are about one-third of that to the PSO model. Of these papers, some showed that the proposed PSO model suitably fitted their experimental data [6–15]. Some further show that PSO model is more suitable than pseudo-first-order model [16–35], IPD model [18,21,23,24,27,33–43], and the Elovich equation [36,42] for this purpose. Only a small number of articles indicated that PSO model is less suitable than other adsorption kinetic models (pseudo-first-order model, IPD model, Elovich equation, etc.). The aforementioned information indicated that PSO model is suitably applied in the analysis of adsorption kinetics, and that its feasibility in engineering applications is worth investigating.

In this work, the time changes of the adsorption of phenol, 4-chlorophenol (4-CP), 2,4-dichlorophenol (2,4-DCP), 2,4,6-trichlorophenol (2,4,6-TCP), and methylene blue (MB) from water were measured using activated carbons prepared from fir wood with KOH activation. The values of PSO model parameters for various adsorption systems were based on the present experimental data, coupled with literature results. Mathematical equations for adsorption kinetics were derived. The characteristic curves were plotted and classified into various zones to infer different levels of adsorption rate. An attempt was made to possibly relate the approaching equilibrium factor and operating time in order to provide a guideline or reference for process design in practical applications.

2. Kinetic model

The PSO model based on adsorption capacity has the form [1–5]:

$$\frac{dq_t}{dt} = k_2(q_e - q_t)^2 \quad (1)$$

where q_t and q_e are the amounts of adsorption at time t and at equilibrium (g/kg), respectively, and k_2 is the PSO rate constant (kg/(g min)). Integrating Eq. (1) and applying the initial conditions, we have:

$$\frac{t}{q_t} = \left(\frac{1}{k_2 q_e^2}\right) + \left(\frac{1}{q_e}\right) t \quad (2)$$

* Corresponding author. Tel.: +886 37 381575; fax: +886 37 332397.
E-mail address: wfc@nuu.edu.tw (F.-C. Wu).

1385-8947/$ – see front matter © 2009 Published by Elsevier B.V.
doi:10.1016/j.cej.2009.02.024

Nomenclature

CP	chlorophenol
d_p	particle size of adsorbent (μm)
DCP	dichlorophenol
HDTMAB	hexadecyltrimethyl ammonium bromide
IPD	intraparticle diffusion
k_2	pseudo-second-order rate constant of adsorption (kg/(g min))
MB	methylene blue
NP	nitrophenol
PHEMA	poly(hydroxyethyl methacrylate)
PSO	pseudo-second-order
q_e	amount of adsorption at equilibrium (g/kg)
q_{ref}	amount of adsorption at $t = t_{ref}$ (g/kg)
q_t	amount of adsorption at time t (g/kg)
Q_t	dimensionless amount of adsorption at time t defined in Eq. (11) (–)
r^2	correlation coefficient (–)
R_w	Approaching equilibrium factor in the PSO model defined in Eq. (5) (–)
t	adsorption time (min)
$t_{0.5}$	half-life of adsorption process, i.e., the time when $q_t = 0.5q_e$ (min)
t_{ref}	longest time of adsorption process (min)
t_x	adsorption time when $q_t = xq_e$ (min)
T	dimensionless adsorption time defined in Eq. (12) (–)
TCP	trichlorophenol
X	fractional adsorption at any time (q_t/q_e) (–)
W	variable ($= X/(1-X)$)

It is noticed that k_2 and q_e in Eq. (2) can be obtained from the intercept and slope in the plot (t/q_t) vs. t.

The above PSO model has been used by many researchers [6–43,46–54]; however, the relationship between PSO rate constant and the characteristic kinetic curve has never been mentioned. Such relationship means that, the characteristics of the Langmuir and Freundlich curves can be described with a separation factor R_L and $1/n$, respectively, in adsorption equilibrium curves [44,45], where R_L and $1/n$ are dimensionless and defined as follows:

$$R_L = \frac{1}{1 + K_L C_0} \tag{3}$$

$$q_e = K_F C_e^{1/n} \tag{4}$$

where K_L and K_F are the Langmuir and Freundlich parameters, respectively. Based on the R_L and $1/n$ values calculated from Eqs. (3) and (4), the Langmuir and Freundlich characteristic curves can be judged [44,45].

Here, an approaching equilibrium factor (R_w), which represents the characteristics of kinetic curve of an adsorption system using the PSO model, is defined as:

$$R_w = \frac{1}{1 + k_2 q_e t_{ref}} \tag{5}$$

$$k_2 q_e t_{ref} = \frac{R_w - 1}{R_w} \tag{6}$$

where t_{ref} is the longest operation time (based on kinetic experiments) in an adsorption system, q_e is the amount of adsorption calculated from Eq. (2). The PSO model is, first, rewritten as:

$$\left(\frac{t_{ref}}{q_{ref}}\right) = \left(\frac{1}{k_2 q_e^2}\right) + \left(\frac{1}{q_e}\right) t_{ref} \tag{7}$$

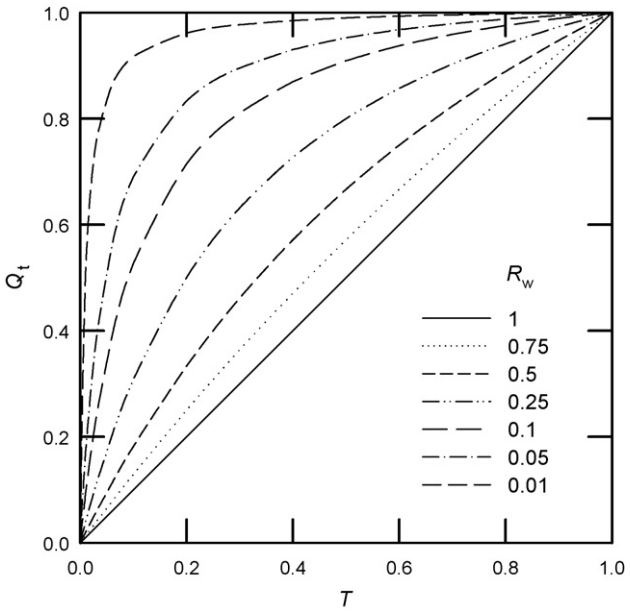

Fig. 1. Characteristic curves of typical pseudo-second-order kinetic model.

where q_{ref} is the amount of adsorption at time t_{ref} (g/kg).

Then, dividing Eq. (2) by Eq. (7) yields:

$$\frac{(t/t_{ref})}{(q_t/q_{ref})} = \frac{(1/k_2 q_e^2) + (t/q_e)}{(1/k_2 q_e^2) + (t_{ref}/q_e)} \tag{8}$$

When both sides of Eq. (8) are multiplier by q_e/t_{ref}, and are combined with Eq. (6), we obtain:

$$\frac{(t/t_{ref})}{(q_t/q_{ref})} = \frac{\left[R_w/(1-R_w)\right] + (t/t_{ref})}{\left[R_w/(1-R_w)\right] + 1} \tag{9}$$

After rearrangement, we have:

$$\frac{q_t}{q_{ref}} = \frac{(t/t_{ref})}{\left[1 - t/t_{ref})\right] R_w + (t/t_{ref})} \tag{10}$$

Defining the dimensionless quantities Q_t and T as follows:

$$Q_t = \frac{q_t}{q_{ref}} \tag{11}$$

$$T = \frac{t}{t_{ref}} \tag{12}$$

inserting Eqs. (11) and (12) into Eq. (10) yields:

$$Q_t = \frac{T}{(1-T)R_w + T} \tag{13}$$

to obtain Q_t of Eq. (13), any one value of parameter R_w that is assumed to be 0.01, 0.05, 0.1, 0.25, 0.75, and 1.00 in Fig. 1, is first fixed. The Q_t values are obtained by replacing T with 0.0 through 1.0. The curve is obtained by plotting Q_t against T for that specific R_w. Fig. 1 shows a family of curves for $R_w = 0.01 - 1.00$. When $R_w = 1$, the kinetic curve is called linear, meaning that $k_2 q_e t_{ref} \ll 1$ in Eq. (3). The possible reasons caused this effect are: (i) it does not facilitate adsorption when the PSO rate constant (k_2) is very small, (ii) the equilibrium amount of adsorption (q_e) is very small, and (iii) the longest time (t_{ref}) of the adsorption process is too short. All these factors indicate an ineffective adsorption system; equilibrium cannot be reached. The curvature of adsorption curve increases as R_w reduces. The characteristic adsorption curve is called approaching equilibrium in the range $1 > R_w > 0.1$; called well approaching

Table 1
The approaching equilibrium factor (R_w) and adsorption kinetic behavior in the PSO model.

R_w value	Type of kinetic curve	Approaching equilibrium level	Zone
$R_w = 1$	Linear	Not approaching equilibrium	0
$1 > R_w > 0.1$	Slightly curved	Approaching equilibrium	I
$0.1 > R_w > 0.01$	Largely curved	Well approaching equilibrium	II
$R_w < 0.01$	Pseudo-rectangular	Drastically approaching equilibrium	III

pseudo equilibrium in the range $0.1 > R_w > 0.01$; and called drastically approaching equilibrium when $R_w < 0.01$. Table 1 summarizes the above-mentioned results.

Seventy-six published articles, which adopted the PSO model, were analyzed and classified as zones I, II, and III, as listed in Tables 2–4, respectively. Zone II contains the most of them, 20 systems, zone III contains next, 15 systems, and zone I contains the least, 9 systems. The meaning of the various zones in adsorption processes is explained in Section 4.3.

3. Materials and methods

3.1. Preparation of activated carbons

Fir wood was dried at 110 °C for 24 h, placed in a sealed ceramic oven, and heated at a rate of 5 °C/min from room temperature to 450 °C. At the same time, N_2 was poured into the oven at a rate of 3 dm^3/min for 1.5 h. Under such oxygen-deficient conditions, the wood was thermally decomposed to porous carbonaceous materials and hydrocarbon compounds. This was the carbonization step.

After the above carbonization step, a char/wood ratio of 0.36 was obtained. The chars of fir wood were removed, crushed, and sieved to a uniform size ranging from 0.83 to 1.65 mm. These powders were then mixed with water and KOH in a stainless steel beaker with a water/KOH/char weight ratio of 2/1/1. After drying at 130 °C for 24 h, the chars were placed in a sealed ceramic oven and heated at a rate of 10 °C/min to 780 °C. The oven was kept at this temperature for 1 h. In the meantime, N_2 gas was flowed into the oven at a rate of 3 dm^3/min. The products were cooled to room temperature and washed with deionized water.

The resulting activated carbon had a BET surface area of 1371 m^2/g, a total pore volume of 0.91 cm^3/g, a micropore volume of 0.74 cm^3/g, and an average pore diameter of 2.4 nm. According to our previous studies on KOH activation of activated carbon [46], the carbon prepared under these conditions were suitable for investigating the adsorption kinetics of phenols and dyes. The activated carbon was crushed and screened into groups of 14–20, 20–30, 30–40, and 40–100 mesh, which was equivalent to the average particle size of 1015, 715, 505, and 285 μm, respectively. Their bulk densities were 0.126, 0.155, 0.127, and 0.123 g/cm^3, respectively.

3.2. Adsorption experiments

The analytical reagent-grade phenol (molecular weight = 94 g/mol), 4-chlorophenol (128.5 g/mol), 2,4-dichlorophenol (163.0 g/mol), 2,4,6-trichlorophenol (197.5 g/mol), and methylene blue (284.3 g/mol) were all offered from Merck Co. The experimental procedures for measuring the adsorption kinetics were the same as those described in previous studies [47,48].

4. Results and discussion

4.1. Suitability of the PSO model

Kinetic results in the adsorption of phenol, 4-CP, 2,4-DCP, and 2,4,6-TCP are shown in Fig. 2a–d. The good linearized plots of t/q_t vs. t according to Eq. (2) indicate the validity of the PSO model. Table 5 lists PSO model parameters of q_e, k_2q_e, R_w, and r^2 (correlation coefficient). Furthermore, r^2 values of IPD model in Table 5 are obtained from the plots of q_t vs. $t^{1/2}$ [33,34] for comparison. The r^2 values from PSO model for the adsorption of phenols vary from 0.98 to 1.0, while the r^2 values from IPD model are lower. However, the adsorption of 2,4,6-TCP on 1015-μm activated carbon is better described by the IPD model ($r^2 = 0.99$). Fig. 3a–d illustrates the good agreement between the measured time changes in the adsorption of phenols and those obtained predicted by the PSO model.

Fig. 4a–c shows the treatment of kinetic data for the adsorption of MB on activated carbon studied. Good linear relationships are obtained for the plots of t/q_t vs. t in Eq. (2) with 285- and 505-μm activated carbons, but poor linear relationships exist with 715- and 1015-μm activated carbons. Linear relationship is good for the plots of q_t vs. $t^{1/2}$ in the IPD model with 505-, 715-, and 1015-μm activated carbons, but slightly poor with 285-μm one. The results in Fig. 4c as well as the r^2 values in Table 5 indicate that both kinetic models describe the adsorption with 285- and 505-μm carbons, whereas IPD model fits the data better with 715- and 1015-μm carbons. The adsorption of two dyes, BV14 and BG4 on 3750-μm resin particles also showed that IPD model better described the adsorption kinetics than PSO model [48]. Thus, the suitability of PSO model should be carefully checked when it is used to describe the adsorption of high-molecular-weight adsorbate on larger adsorbent particles. However, most of the adsorbents used are tiny particles or powders,

Table 2
The PSO approaching equilibrium factors taken from literature (in zone I).

Adsorbate	Adsorbent	q_e (g/kg)	k_2q_e (min^{-1})	t_{ref} (min)	R_w (–)	References
Basic red 46	Clay-wood sawdust	25.9	0.259	30	0.114	[36]
Phenol	Carbonized beet pulp	88.9	0.048	90	0.188	[17]
Basic blue 3	Cyclodextrin polymer	46.1	0.0246	300	0.12	[38]
Basic violet 3	Cyclodextrin polymer	40.4	0.0175	300	0.16	[38]
MB	Dehydrated peanut hull	99	0.0075	1200	0.10	[23]
Atropine	Activated carbon (F400)	18.59	0.0359	140	0.17	[9]
	Activated carbon (F400AN)	18.87	0.0255	140	0.22	
Lysozyme	Dye-affinity adsorbent	666.7	0.0201	120	0.293	[51]
	Poly(glycidyl methacrylate)	317	0.0235	120	0.26	[13]

Table 3
The PSO approaching equilibrium factors taken from literature (in zone II).

Adsorbate	Adsorbent	q_e (g/kg)	k_2q_e (min^{-1})	t_{ref} (min)	R_w (–)	References
Basic violet 3	Palygorskite	33	0.132	290	0.026	[16]
Acid blue	Calcinated colemanite ore waste	53.2	0.056	180	0.090	[18]
Basic violet 14	Peat-resin particle	67.6	0.020	720	0.065	[48]
Basic green 4	Peat-resin particle	69.0	0.014	720	0.088	[48]
MB	Dehydrated wheat bran carbon	52.9	0.010	2000	0.048	[19]
Paraquat	Activated clay (64 μm)	56.2	0.562	60	0.029	[39]
Basic violet 10	Cyclodextrin polymer	32.3	0.0375	300	0.082	[38]
Paraquat	Bleaching earth waste	11.2	0.434	120	0.019	[6]
	Activated clay	33.33	0.967	60	0.017	[7]
Phenol	Activated carbon	7.07	0.206	300	0.016	[39]
Lysozyme	PHEMA/chitosan-dye	80.0	0.112	90	0.090	[20]
	NaY zeolite	17.39	0.360	60	0.044	[22]
Basic blue 9	Cyclodextrin/carboxylic group	39.9	0.096	300	0.034	[8]
4-NP	Bentonite (0.20 mm)	10.2	1.09	80	0.011	[41]
Acid red 274	*Dicranella varia*	1000	0.66	150	0.01	[43]
Methylene green	Commercial activated carbon	0.502	0.192	240	0.021	[24]
Levulinic acid	Basic anion exchangers D301	157.0	0.0595	240	0.065	[52]
Acid orange 51	Eggshell waste	112	0.345	120	0.024	[11]
Dye DR80	Soy meal hull	185	1.63	12	0.049	[28]
Ibuprofen	Commercial activated carbon	85.5	0.1995	360	0.014	[30]

and the molecular weights of adsorbates are not high enough (e.g., phenols and heavy metal ions). The PSO model is thus suitable for common adsorption systems

4.2. Approaching equilibrium factor (R_w) and the rate index (k_2q_e)

The R_w values in the adsorption of phenols on activated carbon are from 0.036 to 0.136 (Table 5), which increase gradually with increasing particle size of adsorbent. In fact, the R_w value was reported to be 0.092, 0.017, and 0.005 in the adsorption of paraquat on activated clay with a particle size of 64, 45, and <37 μm, respectively [49]. Moreover, the R_w value was 0.067, 0.011, and 0.013 in the adsorption of 4-NP on yellow bentonite with a particle size of 75.5, 200, and 400 μm, respectively [41]. In general, the larger the size of adsorbent particles, the more the increase in R_w value and the more difficult it was for the adsorption of adsorbates to approach equilibrium. However, R_w depends not only on particle size of adsorbent but also on the properties of solution, adsorbent, and adsorbate. In our experiments, only particle size was varied while other variables were kept constant. In practice, R_w can be used for various purposes in adsorption systems, for example, to compare adsorbent capability, and to search for suitable adsorbents for specific adsorbates.

Another parameter in the PSO model is k_2q_e (min^{-1}), which can really reflect the kinetic performance. Eq. (1) can be rearranged as:

$$\frac{d(q_t/q_e)}{dt} = k_2q_e\left[1-\left(\frac{q_t}{q_e}\right)\right]^2 \quad (14)$$

Eq. (14) reveals that the time changes in dimensionless solid-phase concentration, $d(q_t/q_e)/dt$, a form of adsorption rate, is proportional to the square of the residual amount of adsorption, $1-(q_t/q_e)$. Consequently, the proportionality constant k_2q_e can be defined as the 2nd-order rate index.

Table 4
The PSO approaching equilibrium factors taken from literature (in zone III).

Adsorbate	Adsorbent	q_e (g/kg)	k_2q_e (min^{-1})	t_{ref} (min)	R_w (–)	References
Basic red 2	Powder acticated carbon	682	1.19	120	0.0070	[53]
Paraquat	Activated bleaching earth	40.3	4.96	120	0.0017	[36]
MB	Palygorskite	48	0.96	120	0.0086	[16]
Malachite green	Thermally treated *Pithophora* sp.	217	1.764	120	0.005	[54]
Paraquat	Activated clay (< 37 μm)	47.2	3.31	60	0.005	[1]
Phenol	Activated carbon	9.64	0.382	300	0.0087	[39]
Basic black	Calcium alginate bead	57.9	0.730	350	0.0039	[21]
4-NP	Bentonite (75.5 μm)	9.90	1.84	80	0.0067	[41]
4-CP	HDTMAB-modified zeolite	1.98	14.0	1440	5.0E−5	[42]
Methylene green	Bagasse fly ash	10.08	0.543	240	0.0076	[24]
Phenol	Dye-affinity adsorbont	15.6	697	60	2.4E−5	[25]
Acid blue 324	*Enteromorpha prolifera*	65.33	8.95	60	0.0019	[10]
Phenols	Activated charcoal	139	1.39	2880	2.5E−4	[12]
Acid blue 92	Soy meal hull	97.1	14.8	12	0.0056	[28]
Ibuprofen	Commercial activated carbon	89.3	0.461	360	0.0060	[30]

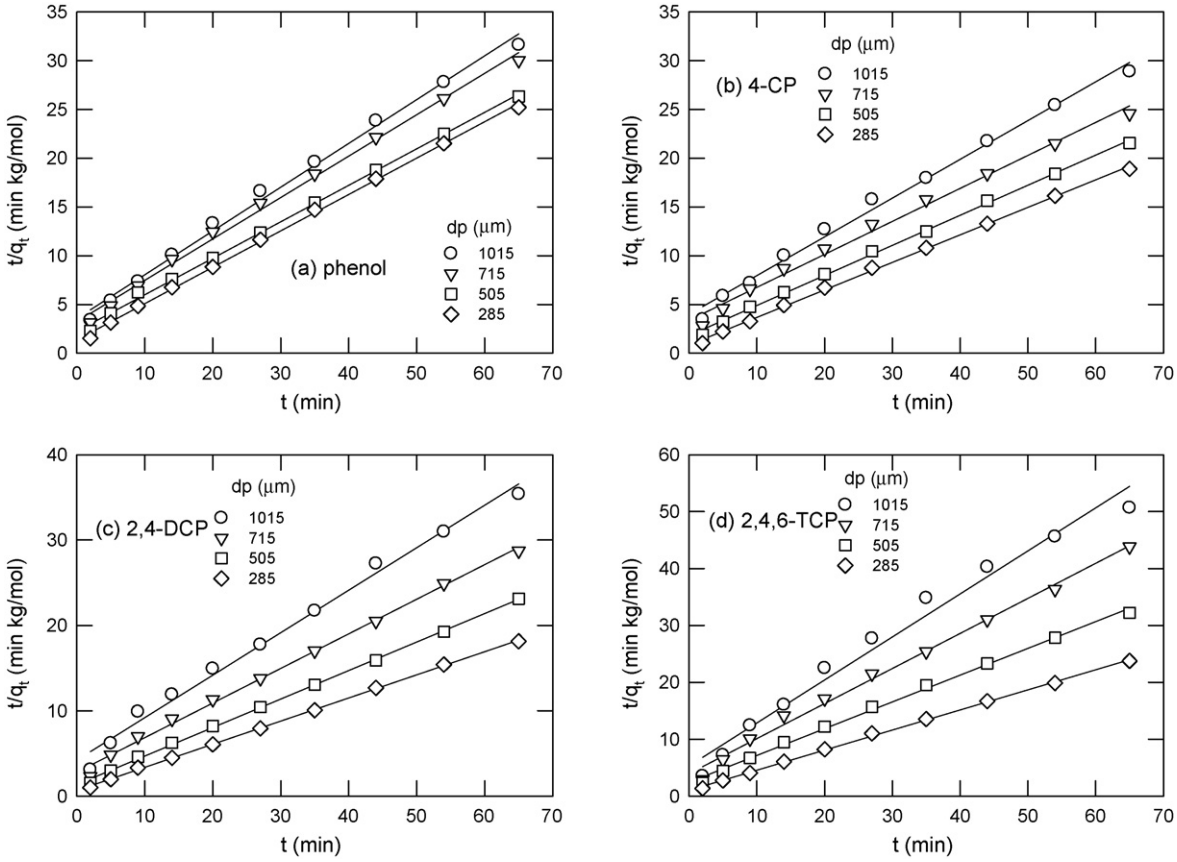

Fig. 2. Application of the pseudo-second-order model to the adsorption of (a) phenol, (b) 4-CP (c) 2,4-DCP, and (d) 2,4,6-TCP on activated carbons with different particle sizes.

There are some drawbacks with R_w in expressing the adsorption rate. For example, $k_2q_e = 11\ min^{-1}$ if the operating time of one system is 9 min, and $k_2q_e = 0.11\ min^{-1}$ if the operating time of another system is 900 min. The R_w values of both systems are actually identical (0.01), but the rate of the former system is much larger than that of the latter system. If 2nd rate index (k_2q_e) is adopted to describe the rate of an adsorption system, the aforementioned problem can be avoided.

On the other hand, Eq. (2) can be rewritten as:

$$\left(\frac{1}{q_t} - \frac{1}{q_e}\right) t = \frac{1}{k_2 q_e^2} \tag{15}$$

Table 5
Kinetic analysis of the adsorption of adsorbates on activated carbons by the PSO and IPD models.

Adsorbate	d_p (μm)	PSO model				IPD model
		q_e (g/kg)	k_2q_e (min^{-1})	R_w (–)	r^2	r^2
Phenol	1015	2.23	0.126	0.109	0.99	0.95
	715	2.36	0.131	0.105	1.00	0.95
	505	2.68	0.165	0.085	1.00	0.91
	285	2.68	0.275	0.053	1.00	0.91
4-CP	1015	2.52	0.0996	0.134	0.99	0.97
	715	2.96	0.100	0.133	0.99	0.98
	505	3.24	0.171	0.083	1.00	0.92
	285	3.54	0.332	0.044	1.00	0.90
2,4-DCP	1015	2.01	0.118	0.115	0.99	0.97
	715	2.47	0.145	0.096	1.00	0.95
	505	2.99	0.246	0.059	1.00	0.90
	285	3.69	0.412	0.036	1.00	0.84
2,4,6-TCP	1015	1.32	0.142	0.098	0.98	0.99
	715	1.62	0.157	0.089	0.99	0.97
	505	2.12	0.193	0.074	1.00	0.94
	285	2.83	0.343	0.043	1.00	0.87
MB	1015	0.368	0.0295	0.343	0.88	0.99
	715	0.469	0.0318	0.326	0.91	0.99
	505	0.634	0.0531	0.225	0.98	0.99
	285	0.817	0.0697	0.181	0.99	0.98

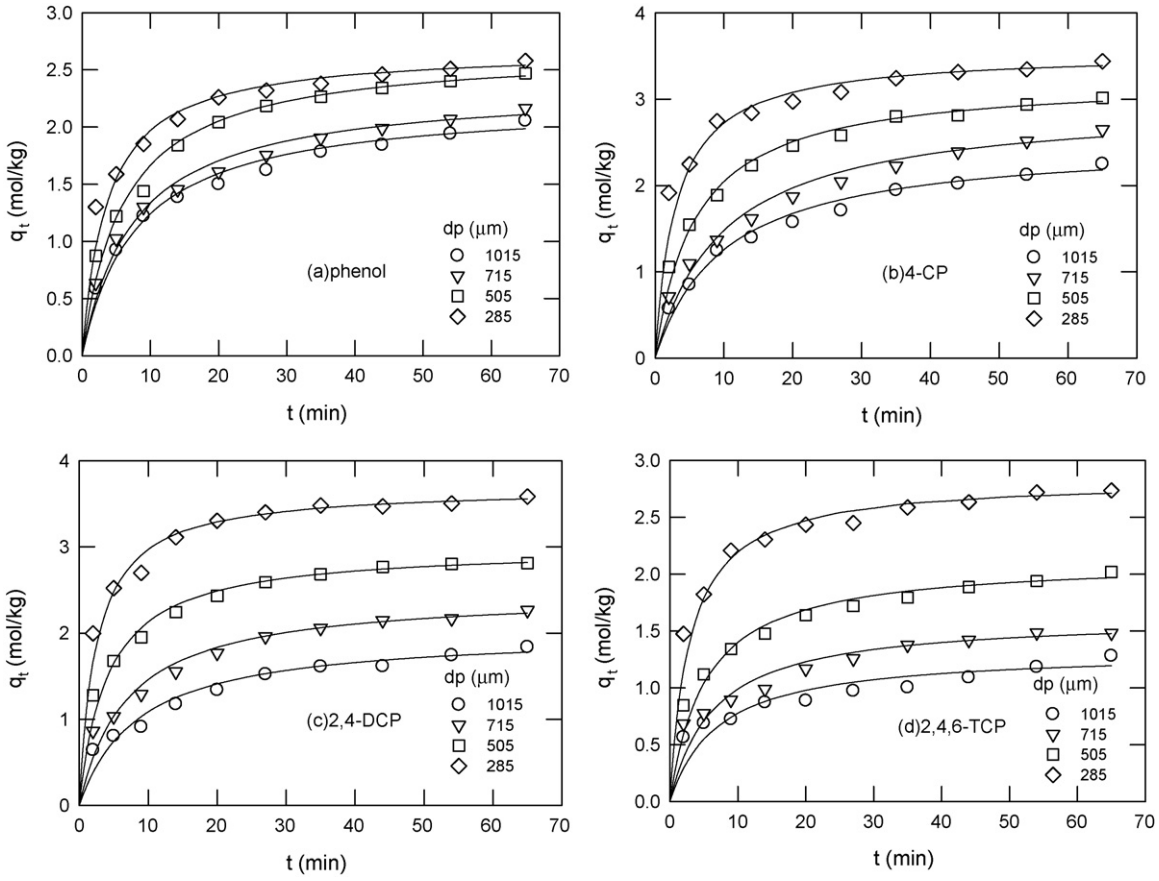

Fig. 3. Adsorption kinetics of (a) phenol, (b) 4-CP (c) 2,4-DCP, and (d) 2,4,6-TCP on activated carbons with different particle sizes (the solid curves were calculated by the pseudo-second-order model).

and

$$t = \frac{\left[q_t/(q_e - q_t)\right]}{k_2 q_e} \tag{16}$$

At the half-life of adsorption process (i.e., $t = t_{0.5}$), we have $q_t = 0.5q_e$ and

$$t_{0.5} = \frac{1}{k_2 q_e} \tag{17}$$

It is evident that k_2q_e is the only parameter of Eq. (17). The k_2q_e value is equal to the inverse of the half-life of adsorption process, describing the actual meaning of 2nd-order adsorption parameter better.

Fig. 5 shows the relationship between k_2q_e and d_p for the activated carbons used. In the adsorption of phenols, k_2q_e is larger for the carbons with smaller particle sizes, and k_2q_e decreases with increasing particle size. When particle size is larger than 715 μm, k_2q_e reaches a plateau. The value of k_2q_e in the adsorption of MB is less than those obtained for the four phenols.

4.3. Adsorption characteristic curves

Usually, commercially available activated carbons are sold with the data of BET surface area, methylene blue value, and iodine value. However, this is not enough from the viewpoint of engineering design. The relationship between accurate operating time and amount of adsorption is needed. Graphical representation of approaching equilibrium factor (R_w) can provide the characteristic curve relating to operating time and amount of adsorption. This kind of adsorption characteristic curve looks like the pump characteristic curve, which provides information under various operating conditions. For example, the adsorption characteristic curve with 505-μm activated carbon is shown in Fig. 6a. Curvatures of the characteristic curves for phenols are larger than their R_w values in zone II, and that for MB is smaller in zone I. Adsorption characteristic curves highlight the relationship between the amount of adsorption and operating time in the adsorption of adsorbates on various adsorbents. Such practical messages are more useful in engineering design.

Only 20% of the published articles that surveyed here belong to zone I (see Tables 2–4). This is because powdered adsorbents are used in most (R_w is small). However, a larger adsorbent is needed to facilitate the followed separation from the liquid. In this case, R_w is larger. Fig. 6b shows that the curvature decreases with increasing particle size, and the adsorption curve is shifted from zone II to zone I. When the adsorption curve belongs to zone I, the relationship between operating time and amount of adsorption is an important factor in engineering practice.

Eq. (16) can be rewritten as:

$$t_x = \frac{W}{k_2 q_e} \tag{18}$$

where $W = q_t/(q_e - q_t)$.

Define the fractional adsorption $X = q_t/q_e$ and let $W = X/(1 - X)$. At equilibrium, $q_t/q_e = 1$, W = infinite, and t_x = infinite. Fig. 7 shows the relationship between W and X values. As X equals 1, W approaches infinite. When X is gradually approaching 1, W and t_x increase rapidly. Engineers must consider both X and t_x values to make

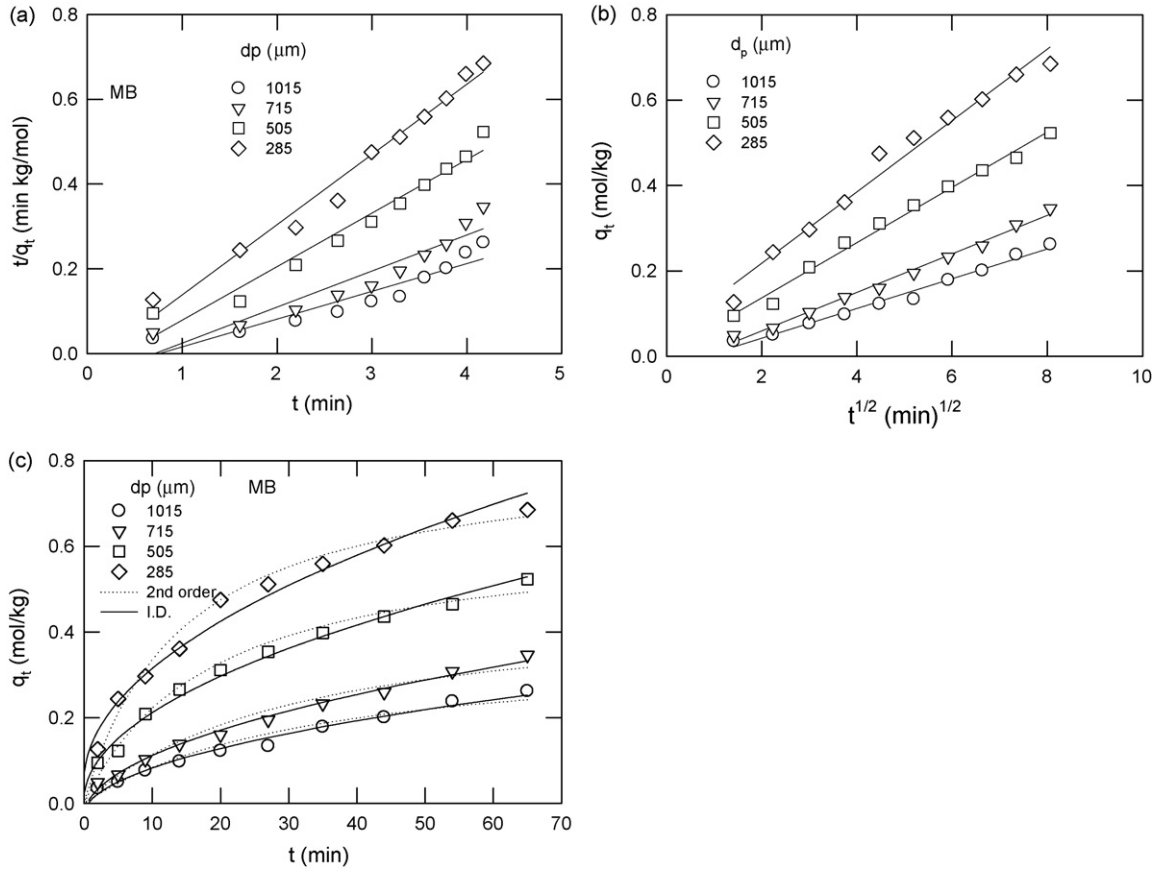

Fig. 4. Kinetics of MB adsorption on activated carbons with different particle sizes (the curves were fitted by (a) the pseudo-second-order model and (b) the intraparticle diffusion model).

suitable decision. Usually, t_x value of an adsorption system can be adopted at $X = 0.95$ on the turning point of the curve shown in Fig. 7.

However, the operation should be carefully selected according to actual experimental conditions. Table 6 lists the required times under various approaching X values for the activated carbons used. For example, the values of $t_{0.6}$, $t_{0.8}$, $t_{0.9}$, $t_{0.95}$, and $t_{0.97}$ for the adsorption of 2,4-DCP on 715-μm activated carbon are 10.3, 27.6, 62.1, 131, and 223 min, respectively. If X increases from 0.6 to 0.8, the amount of adsorption increases by 20% and, in the mean time, a 17.3-min increase in operating time is found. This kind of alter-

Table 6
Relationship between approaching equilibrium factor and operating time studied.

Adsorbate	d_p (μm)	$k_2 q_e$ (min^{-1})	$X = 0.6$	$X = 0.8$	$X = 0.9$	$X = 0.95$	$X = 0.97$
			$t_{0.6}$ (min)	$t_{0.8}$ (min)	$t_{0.9}$ (min)	$t_{0.95}$ (min)	$t_{0.97}$ (min)
Phenol	1015	0.126	11.9	31.7	71.4	151	257
	715	0.131	11.5	30.5	68.7	145	247
	505	0.165	9.09	24.2	54.5	115	196
	285	0.275	5.45	14.5	32.7	69.1	118
4-CP	1015	0.099	15.1	40.1	90.4	191	325
	715	0.100	15.0	40.0	90.0	190	323
	505	0.171	8.77	23.4	52.6	111	189
	285	0.332	4.52	12.0	27.1	57.2	97.4
2,4-DCP	1015	0.118	12.7	33.9	76.3	161	274
	715	0.145	10.3	27.6	62.1	131	223
	505	0.246	6.10	16.3	36.5	77.2	131
	285	0.412	3.64	9.71	21.8	46.1	78.5
2,4,6-TCP	1015	0.142	10.6	28.2	63.4	134	228
	715	0.157	9.55	25.5	57.3	121	206
	505	0.193	7.77	20.7	46.6	98.4	168
	285	0.343	4.37	11.7	26.2	55.4	94.3
MB	1015	0.0295	50.8	136	305	644	1095
	715	0.0318	47.2	126	283	597	1018
	505	0.0531	28.2	75.3	169	358	609
	285	0.0697	21.5	57.4	129	273	464

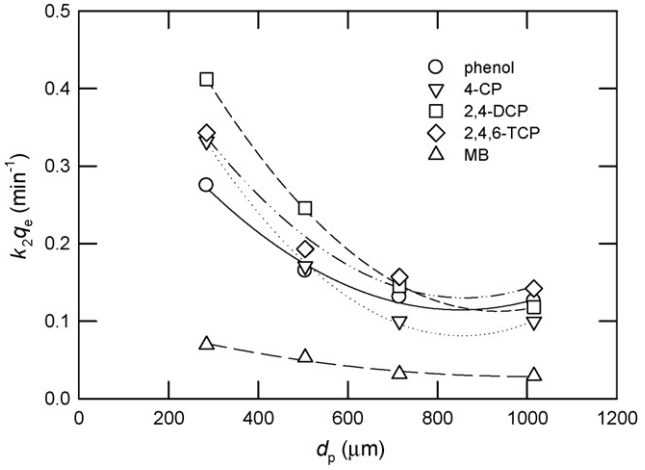

Fig. 5. The 2nd-order rate index in the adsorption of phenols and MB on activated carbons with different particle sizes.

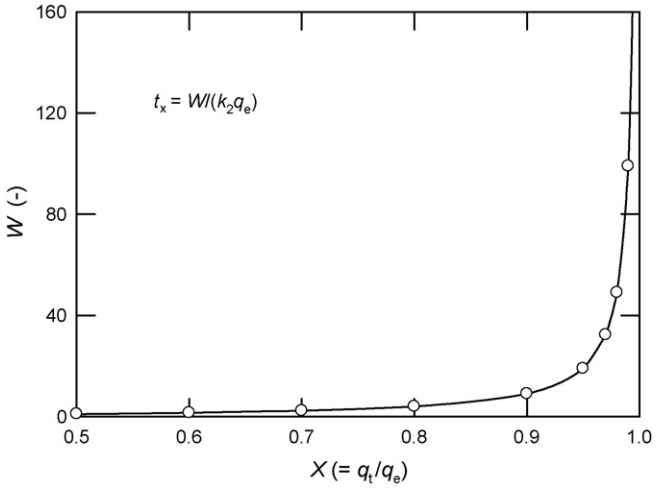

Fig. 7. Relationship between the fractional adsorption X (= q_t/q_e) and the value of W (= $X/(1-X)$).

ation would be acceptable. But, the amount of adsorption increases by 2% only and a 92-min increase in operating time is found if X increases from 0.95 to 0.97. In this case, the economic implication should be evaluated. Thus, the most suitable X value should be determined based on actual operating conditions in engineering practice.

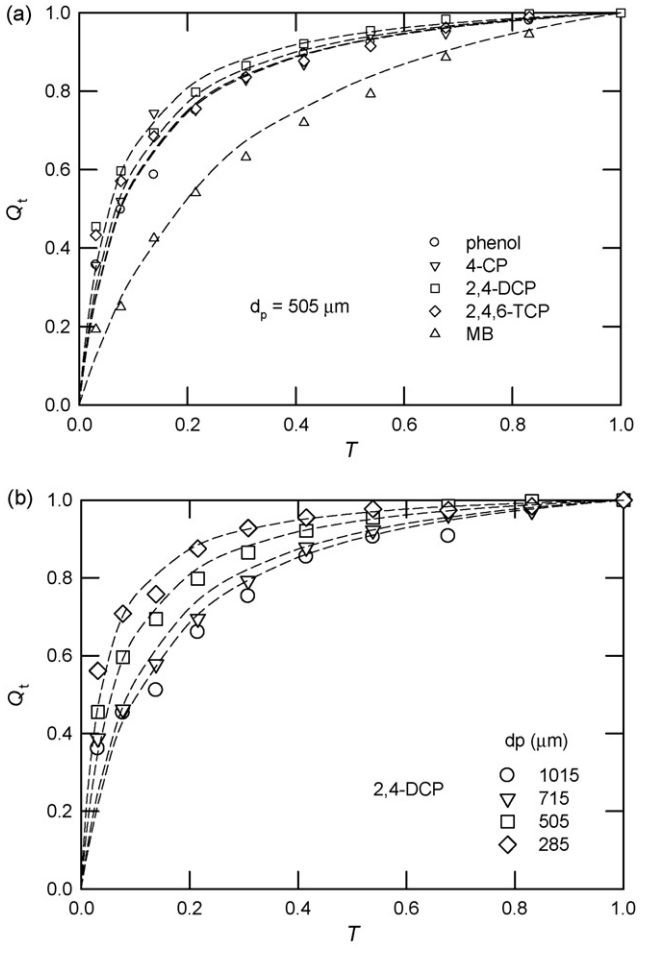

Fig. 6. Characteristic curves in the adsorption of various phenols and MB on activated carbons with different particle sizes.

5. Conclusions

The suitability of the pseudo-second-order model for liquid-phase adsorption processes has been investigated. In addition to the adsorption of phenol, 4-CP, 2,4-DCP, 2,4,6-TCP, and MB on KOH-activated carbons under controlled conditions, literature results were also surveyed and analyzed. The following results were obtained.

1. The plots between dimensionless amount of adsorption (Q_t) and the approaching equilibrium factor (R_w) in PSO model were characteristic of adsorption processes. According to R_w values, the characteristic curves were classified into three zones: $1 > R_w > 0.1$ (zone I), $0.1 > R_w > 0.01$ (zone II), and $R_w < 0.01$ (zone III). Fifty-five percent of the published articles surveyed were belonged to zone II. The characteristic curves could be used to describe the adsorption kinetics, and to facilitate a more accurate inference in adsorbent selection for engineering practice.
2. The PSO model well fitted the experimental data of phenols studied, but this is only the case for the data of MB with 285- and 505-μm carbons. The results of MB with 715- and 1015-μm carbons were well fitted by intraparticle diffusion model. This meant that the PSO model was suitable for the adsorption of lower molecular-weight adsorbates on smaller adsorbent particles.
3. The newly defined second-order rate index, k_2q_e, was more suitable to describe the adsorption kinetics than the approaching equilibrium factor R_w. In this manner, the changes of the amount of adsorption on an adsorbent with time could be readily followed.

Acknowledgment

Financial support of this work by the National Science Council, ROC under contract no. NSC 96-2221-E-239-021 is gratefully acknowledged.

References

[1] Y.S. Ho, G. McKay, Comparative sorption kinetics studies of dyes and aromatic compounds onto fly ash, J. Environ. Sci. Health A34 (1999) 1179–1204.
[2] G. McKay, Y.S. Ho, J.C.Y. Ng, Biosorption of copper from waste waters: a review, Sep. Pur. Methods 28 (1999) 87–125.
[3] G. McKay, Y.S. Ho, The sorption of lead(II) ions on peat, Water Res. 33 (1999) 578–584.

[4] G. McKay, Y.S. Ho, Pseudo-second order model for sorption processes, Process Biochem. 34 (1999) 451–465.
[5] Y.S. Ho, G. McKay, A kinetic study of dye sorption by biosorbent waste product pith, Resources, Conservation and Recycling 25 (1999) 171–193.
[6] W.T. Tsai, C.W. Lai, Adsorption of herbicide paraquat by clay mineral regenerated from spent bleaching earth, J. Hazard. Mater. 134 (2006) 144–148.
[7] W.T. Tsai, C.W. Lai, K.J. Hsien, The effects of pH and salinity on kinetics of paraquat sorption onto activated clay, Colloids Surf. A Physicochem. Eng. Aspects 224 (2003) 99–105.
[8] G. Crini, H.N. Peindy, Adsorption of C.I. Basic blue 9 on cyclodextrin-based material containing carboxylic groups, Dyes Pigments 70 (2006) 204–211.
[9] P. Chingombe, B. Saha, R.J. Wakeman, Sorption of atrazine on conventional and surface modified activated carbons, J. Colloid Interface Sci. 302 (2006) 408–416.
[10] A. Ozer, A. Gonul, M. Turabik, The biosorption of Acid red 337 and Acid blue 324 on *Enteromorpha prolifera*: the application of nonlinear regression analysis to dye biosorption, Chem. Eng. J. 112 (2005) 181–190.
[11] W.T. Tsai, K.J. Hsien, H.C. Hsu, C.M. Lin, K.Y. Lin, C.H. Chiu, Utilization of ground eggshell waste as an adsorbent for removal of dyes from aqueous solution, Bioresour. Technol. 99 (2008) 1623–1629.
[12] M.L. Soto, A. Moure, H. Dominguez, J.C. Parajo, Charcoal adsorption of phenolic compounds present in distilled grape pomace, J. Food Eng. 84 (2008) 156–163.
[13] E.B. Altintas, N. Tuzmen, N. Candan, A. Denizli, Use of magnetic poly(glycidylmethacrylate) monosize beads for the purification of lysozyme in batch system, J. Chromatogr. B 853 (2007) 105–113.
[14] G.C. Panda, S.K. Das, T.S. Bandopadhyay, A.K. Guha, Adsorption of nickel on husk of *Lathyrus sativus*: behavior and binding mechanism, Colloids Surf. B 57 (2007) 135–142.
[15] R.S. Juang, F.C. Wu, R.L. Tseng, Solute adsorption and enzyme immobilization on chitosan beads prepared from shrimp shell wastes, Bioresour. Technol. 80 (2001) 187–193.
[16] A. Al-Futaisi, A. Jamrah, R. Al-Hanai, Aspects of cationic dye molecule adsorption to palygorskite, Desalination 214 (2007) 327–342.
[17] G. Dursun, H. Cicek, A.Y. Dursun, Adsorption of phenol from aqueous solution by using carbonized beet pulp, J. Hazard. Mater. 125 (2005) 175–182.
[18] N. Atar, A. Olgun, Removal of acid blue 062 on aqueous solution using calcinated colemanite ore waste, J. Hazard. Mater. 146 (2007) 171–179.
[19] A. Ozer, G. Dursun, Removal of methylene blue from aqueous solution by dehydrated wheat bran carbon, J. Hazard. Mater. 146 (2007) 262–269.
[20] G. Bayramoglu, B. Kaya, M.Y. Arica, Procion Brown MX-5BR attached and Lewis metals ion-immobilized poly(hydroxyethyl methacrylate)/chitosan IPNs membranes: their lysozyme adsorption equilibria and kinetics characterization, Chem. Eng. Sci. 57 (2002) 2323–2334.
[21] R. Aravindhan, N.N. Fathima, J.R. Rao, B.U. Nair, Equilibrium and thermodynamic studies on the removal of basic black dye using calcium alginate beads, Colloids Surf. A Physicochem. Eng. Aspects 299 (2007) 232–238.
[22] Y.K. Chang, L. Chu, J.C. Tsai, S.J. Chiu, Kinetic study of immobilized lysozyme on extrudate-shaped NaY zeolite, Process Biochem. 41 (2006) 1864–1874.
[23] D. Ozer, G. Dursun, A. Ozer, Methylene blue adsorption from aqueous solution by dehydrated peanut hull, J. Hazard. Mater. 144 (2007) 171–179.
[24] I.D. Mall, V.C. Srivastava, N.K. Agarwal, Adsorptive removal of auramine-O: kinetic and equilibrium study, J. Hazard. Mater. 143 (2007) 386–395.
[25] S. Senel, A. Kara, G. Alsancak, A. Denizli, Removal of phenol and chlorophenols from water with reusable dye-affinity hollow fibers, J. Hazard. Mater. 138 (2006) 317–324.
[26] M. Kilic, M.E. Keskin, S. Mazlum, N. Mazlum, Effect of conditioning for Pb(II) and Hg(II) biosorption on waste activated sludge, Chem. Eng. Process. 47 (2008) 31–40.
[27] J.G. Cai, A.M. Li, H.Y. Shi, Z.H. Fei, C. Long, Q.X. Zhang, Equilibrium and kinetic studies on the adsorption of aniline compounds from aqueous phase onto bifunctional polymeric adsorbent with sulfonic groups, Chemosphere 61 (2005) 502–509.
[28] M. Arami, N.Y. Limaee, N.M. Mahmoodi, N.S. Tabrizi, Equilibrium and kinetics studies for adsorption of direct and acid dyes from aqueous solution by soy meal hull, J. Hazard. Mater. 135 (2006) 171–179.
[29] G.C. Panda, S.K. Das, S. Chatterjee, P.B. Maity, T.S. Bandopadhyay, A.K. Guha, Adsorption of cadmium on husk of *Lathyrus sativus*: physicochemical study, Colloids Surf. A. Physciochem. Eng. Aspects 50 (2006) 49–54.
[30] A.S. Mestre, J. Pires, J.M.F. Nogueira, A.P. Carvalho, Activated carbons for the adsorption of ibuprofen, Carbon 45 (2007) 1979–1988.
[31] D.P. Mungasavalli, T. Viraraghavan, Y.C. Jin, Biosorption of chromium from aqueous solutions by pretreated *Aspergillus niger*: batch and column studies, Colloids Surf. A Physicochem. Eng. Aspects 301 (2007) 214–223.
[32] B.Y.M. Bueno, M.L. Torem, F. Molina, L.M.S. Bueno, B.Y.M. de Mesquita, Biosorption of lead(II), chromium(III) and copper(II) by *R. opacus*: equilibrium and kinetic studies, Miner. Eng. 21 (2008) 65–75.
[33] R.S. Juang, F.C. Wu, R.L. Tseng, Mechanism of adsorption of phenols and dyes from water using activated carbons prepared from plum kernels, J. Colloid Interface Sci. 227 (2000) 437–444.
[34] F.C. Wu, R.L. Tseng, R.S. Juang, Kinetic modeling of liquid-phase adsorption of reactive dyes and metal ions on chitosan, Water Res. 35 (2001) 613–618.
[35] R.L. Tseng, S.K. Tseng, Pore structure and adsorption performance of KOH-activated carbons prepared from corncob, J. Colloid Interface Sci. 287 (2005) 428–437.
[36] W.T. Tsai, C.W. Lai, K.J. Hsien, Adsorption kinetics of herbicide paraquat from aqueous solution onto activated bleaching earth, Chemosphere 55 (2004) 829–837.
[37] N. Unlu, M. Ersoz, Adsorption characteristics of heavy metal ions onto a low cost biopolymeric sorbent from aqueous solutions, J. Hazard. Mater. 136 (2006) 272–280.
[38] G. Crini, Kinetic and equilibrium studies on the removal of cationic dyes from aqueous solution by adsorption onto a cyclodextrin polymer, Dyes Pigments 77 (2008) 415–426.
[39] V.C. Srivastava, M.M. Swamy, I.D. Mall, B. Prasad, I.M. Mishra, Adsorptive removal of phenol by bagasse fly ash and activated carbon: equilibrium, kinetics and thermodynamics, Colloids Surf. A Physicochem. Eng. Aspects 272 (2006) 89–104.
[40] F. Cicek, D. Ozer, A. Ozer, A. Ozer, Low cost removal of reactive dyes using wheat bran, J. Hazard. Mater. 146 (2007) 408–416.
[41] Z. Yaneva, B. Koumanova, Comparative modelling of mono- and dinitrophenols sorption on yellow bentonite from aqueous solutions, J. Colloid Interface Sci. 293 (2006) 303–311.
[42] A. Kuleyin, Removal of phenol and 4-chlorophenol by surfactant-modified natural zeolite, J. Hazard. Mater. 144 (2007) 307–315.
[43] G. Akkaya, A. Ozer, Biosorption of Acid Red 274 on *Dicranella varia*: determination of equilibrium and kinetic model parameters, Process Biochem. 40 (2005) 3559–3568.
[44] F.C. Wu, R.L. Tseng, Liquid-solid phase countercurrent multi-stage adsorption process using the Langmuir equation, J. Hazard. Mater. 155 (2008) 449–458.
[45] R.L. Tseng, F.C. Wu, Inferring the favorable adsorption level and the concurrent multi-stage process with the Freundlich constant, J. Hazard. Mater. 155 (2008) 277–287.
[46] F.C. Wu, R.L. Tseng, R.S. Juang, Preparation of highly microporous carbons from fir wood by KOH activation for adsorption of dyes and phenols from water, Sep. Purif. Technol. 47 (2005) 10–19.
[47] F.C. Wu, R.L. Tseng, C.C. Hu, Comparison of properties and adsorption performance of KOH-activated and steam-activated carbons, Microporous Mesoporous Mater. 80 (2005) 95–106.
[48] Q. Sun, L. Yang, The adsorption of basic dyes from aqueous solution on modified peat-resin particle, Water Res. 37 (2003) 1535–1544.
[49] W.T. Tsai, C.W. Lai, K.J. Hsien, Effect of particle size of activated clay on the adsorption of paraquat from aqueous solution, J Colloid Interface Sci. 263 (2003) 29–34.
[50] R.R. Sheha, E. Metwally, Equilibrium isotherm modeling of cesium adsorption onto magnetic materials, J. Hazard. Mater. 143 (2007) 354–361.
[51] E.B. Altintas, A. Denizil, Monosize poly(glycidylmethacrylate) beads for dye-affinity purification of lysozyme, Int. J. Biol. Macromol. 38 (2006) 99–106.
[52] B.J. Liu, Q.L. Ren, Sorption of levulinic acid onto weakly basic anion exchangers: equilibrium and kinetic studies, J. Colloid Interface Sci. 294 (2006) 281–287.
[53] K.V. Kumar, Pseudo-second order models for the adsorption of safranin onto activated carbon: comparison of linear and non-linear regression methods, J. Hazard. Mater. 142 (2007) 564–567.
[54] K.V. Kumar, S. Sivanesan, V. Ramamurthi, Adsorption of malachite green onto *Pithophora* sp., a fresh water algae: equilibrium and kinetic modeling, Process Biochem. 40 (2005) 2865–2872.